SMAR 2017 – Fourth Conference on Smart Monitoring,
Assessment and Rehabilitation of Civil Structures

SMAR 2017

Nonlinear Analysis of Hollow-Core Composite Building Columns

Mohanad M. Abdulazeez[1], Mohamed A. ElGawady[2]

[1] Graduate Research Assistance and PhD student, Dept. of Civil, Architectural, and Environmental Engineering, Missouri University of Science and Technology, Rolla, MO. 65409

[2] Benavides Associate Professor, Dept. of Civil, Architectural, and Environmental Engineering, Missouri University of Science and Technology, Rolla, MO. 65409

ABSTRACT

This paper numerically investigates the behavior of hollow-core fiber-reinforced polymer-concrete-steel (HC-FCS) building columns under combined axial compression and flexural loadings. The HC-FCS column for buildings consists of an outer circular fiber-reinforced polymer (FRP) tube, an inner square steel tube, and a concrete wall between them. A three-dimensional numerical model has been developed using LS_DYNA software for modeling of large scale HC-FCS columns. The nonlinear FE models were designed and validated against experimental results gathered from HC-FCS columns tested under cyclic lateral loading. The FE results were in decent agreement with the experimental backbone curves. These models subsequently were used to conduct a parametric study investigating the effects of the concrete wall thickness, steel tube width-to-thickness (B/t) ratio, and local buckling instability on the behavior of the HC-FCS columns. The obtained local buckling stresses results from the FE models were compared with the values calculated from the empirical equations of the available design codes. Finally, an approximated expression based on the available empirical formulas and the FE model results has been proposed in this paper to calculate the local buckling stresses of HC-FCS columns.

INTRODUCTION

Concrete-filled steel tubes (CFST) have been considered a good alternative type for high-performance structural elements since they were first developed by Montague (1978) in the late 1980s (Shakir-Khalil and Illouli 1989). A CFST consists of a hollow steel tube filled with concrete with or without internal steel–reinforcing bars. Two cross-sections of steel tubes are commonly used in the construction of CFST: circular and rectangular.

More recently, a different version of hollow-core columns was proposed where the outer steel tube was replaced with FRP tube (Teng and Lam 2004). The FRP tube fibers are mostly oriented in the hoop direction to increase the confinement of the concrete wall.

Herein and after, will be referred to as hollow-core fiber-reinforced polymer-concrete-steel (HC-FCS) columns. Many studies have been conducted to investigate the flexural behavior, axial compressive behavior, and combined axial-flexural behavior of the HC-FCS columns (Abdelkarim and ElGawady 2014; Abdelkarim and ElGawady 2016; Abdelkarim et al. 2016; Abdelkarim et al. 2015; Abdulazeez et al. 2017; Fam and Rizkalla 2001; Mirmiran and Shahawy 1997; Ozbakkaloglu and Akin 2011; Ozbakkaloglu and Saatcioglu 2007; Youssf et al. 2014; Zhang et al. 2012). These studies demonstrated that HC-FCS columns can display superior performance under extreme loads as the concrete wall is continuously confined by both the outer FRP tube and inner steel tube, which results in a triaxial state of compression for the concrete shell that increases the strength and strain capacity of the concrete. Furthermore, local and global buckling of the steel tube is restrained by the concrete wall, thereby increasing the deformation and strength capacity of an HC-FCS member.

There are two types of buckling analysis, linear buckling analysis (eigenvalue) and nonlinear buckling analysis (post-buckling). Methods and formulas are widely available for calculating the buckling in this linear stage based on experimental results.
Experimental and theoretical studies have been conducted on bare steel tubes and concrete-filled box steel tube (CFBST) columns to investigate the behavior and accuracy of the local buckling instabilities (AISC 2010; Cheung 1976; Uy 1998; Uy and Bradford 1996; Von Karman et al. 1932; Winter 1970; Wright 1995). The theoretical solutions in these studies were developed to ascertain the initial local and post local buckling and relied mostly on the use of two methods: finite strip method (FSM) and effective width method (EWM).
The FSM was introduced by Cheung (1976) and then developed through invoking the semi-analytical finite strip method (SAFSM) by Uy and Bradford (1996); Uy (1998). This method was used in the initial local buckling capacity calculations by incorporating the effect of the residual stresses, which can be important in the elastic range of structural response (Uy 2001).
The concept of EWM was first proposed by Von Karman et al. (1932) for perfect plates, which accounts for post-buckling of stiffened plate elements by suggesting that the concentration of the design stresses distribution was mainly supported edge portions. This method was then modified by Winter (1974, 1968) to account for the reduction in real plates strength due to the effect of the imperfection.
The finite-element (FE) method offers an approach to investigate the behavior of HC-FCS columns where the confinement pressure is not uniform. Recently, Abdelkarim and ElGawady (2015) have developed FE models to investigate the lateral behavior of HC-FCS columns having a circular steel core with FRP tubes. This paper extends Abdelkariem's work to investigate the behavior of HC-FCS with inner rectangular steel cross section and outer circular FRP section investigated under constant axial compression load and lateral loads. This paper reports the results of a parametric study in which the FE method was employed using LS_DYNA software, which is a multi-purpose explicit and implicit finite element software.

FE MODELING AND PARAMETRIC STUDY

An HC-FCS column with square inner steel tube specimen called DST-8 was tested by Ozbakkaloglu and Idris (2014) and used for the model validation in this study. The cross-section of the tested column had an outer Aramid fiber reinforced polymer (AFRP) tube diameter (D) of 150 mm and a height of 1200 mm from the footing top surface. The inner square steel tube had a cross section width (B) of 89 mm. The column was tested as a free cantilever under combined constant axial compressive load and cyclic lateral load. The lateral load was applied at a height of 1000 mm from the footing top level, resulting in a shear span-to-diameter ratio (M/VD) of 6.7, where M and V are the ultimate moment and shear at the bottommost section of the column, respectively, and D is the cross section diameter. The symmetry of the tested column within the vertical plane allowed modeling of only half of the column.
The footing, concrete wall, and loading stub were modeled using solid elements with an average length of 20 mm and constant-stress one-point quadrature integration to reduce the computational time and increase the model stability. The outer FRP and inner steel tubes were simulated using shell elements with an average height of 25 mm. The hourglass type and coefficient used during this study were 5 and 0.03, respectively.
The column DST-8 was tested as a cantilever member, and the lateral load was monotonically applied at a height 1000 mm from the footing's top level. In the FE model, the load was incrementally applied using a displacement control regime. Figure 1 shows the moments at the bottommost section of the column and the middle of the stub lateral displacements for the columns obtained from experimental work and FE model.

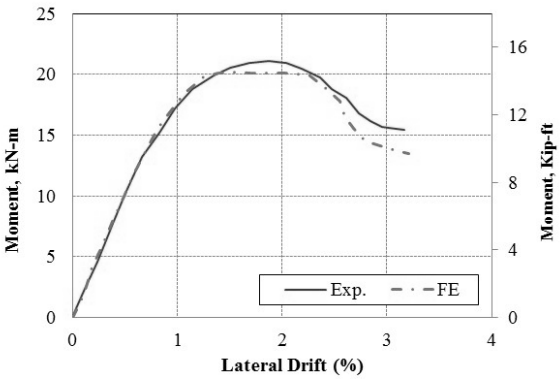

Figure 1. Experimental (Ozbakkaloglu and Idris 2014) versus FE lateral drift-moment backbone curve for specimens: DST-8.

As shown in Figure 1, the FE predicted the performance of the column with high accuracy. The model predicted 94% and 96.5% of the moment and ultimate displacement measured during the experimental work, respectively. The FE model predicted a high-stress concentration at the bottom 50 mm of the AFRP layer above the footing level ending with the AFRP shell failure (Fig. 2). Similar failure behavior displayed during the experimental work of the tested column. Once the model was validated in the current study as well as in Abdelkarim and ElGawady (2015), a comprehensive parametric study was carried out to provide an in-depth understanding of the performance of full-scale HC-FCS columns with rectangular inner steel tubes and the main parameters that control their performance. Table 1 shows the material and geometrical properties of the investigated HC-FCS column models in this study. The reference column model (C0 in Table 1) had an outer diameter (D) of 1,524 mm, inner square tube width (B) of 712 mm, and a height (H) of 10,160 mm from the footing top face. The lateral load was applied at a height of 7,620 mm from the footing top level, resulting in an M/VD of 5 (Fig. 3). The symmetry of the tested column within the vertical plane allowed modeling of only half of the column.

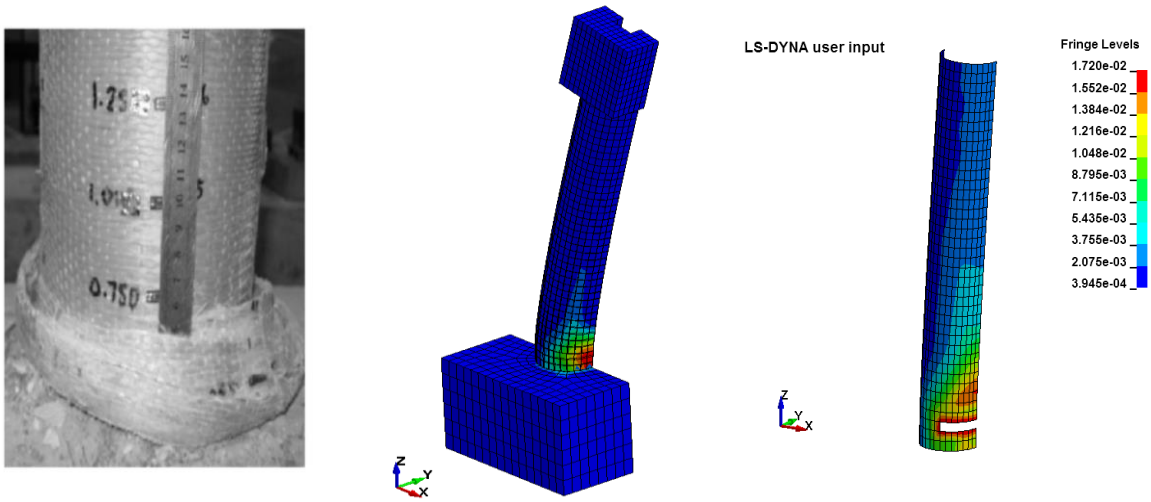

(a) (b)

Figure 2. Rupture of FRP tube (a) tested column (Ozbakkaloglu and Idris 2014); (b) FE results for the AFRP failure.

Table 1. Summary of the parametric study models

Group	Model Name	Parameter	Details	Height H, [mm]	Outer diameter D, [mm]	Steel tube width B, [mm]	FRP tube thickness t_f, [mm]	Concrete wall thickness t_c, [mm]	Steel tube thickness t, [mm]
A	C1	Concrete Wall Thickness t_c, [mm]	152.4	10,160	1,524	864	8.5	152.4	7.3
	C2		203.2			788		203.2	6.63
	C0		254			712		254	6
	C3		305			635		305	5.42
	C4		381			539		381	4.5
B	C5	B/t	30	10,160	1,524	712	8.5	254	24
	C6		60						12
	C7		90						8
	C0		120						6
	C8		180						4

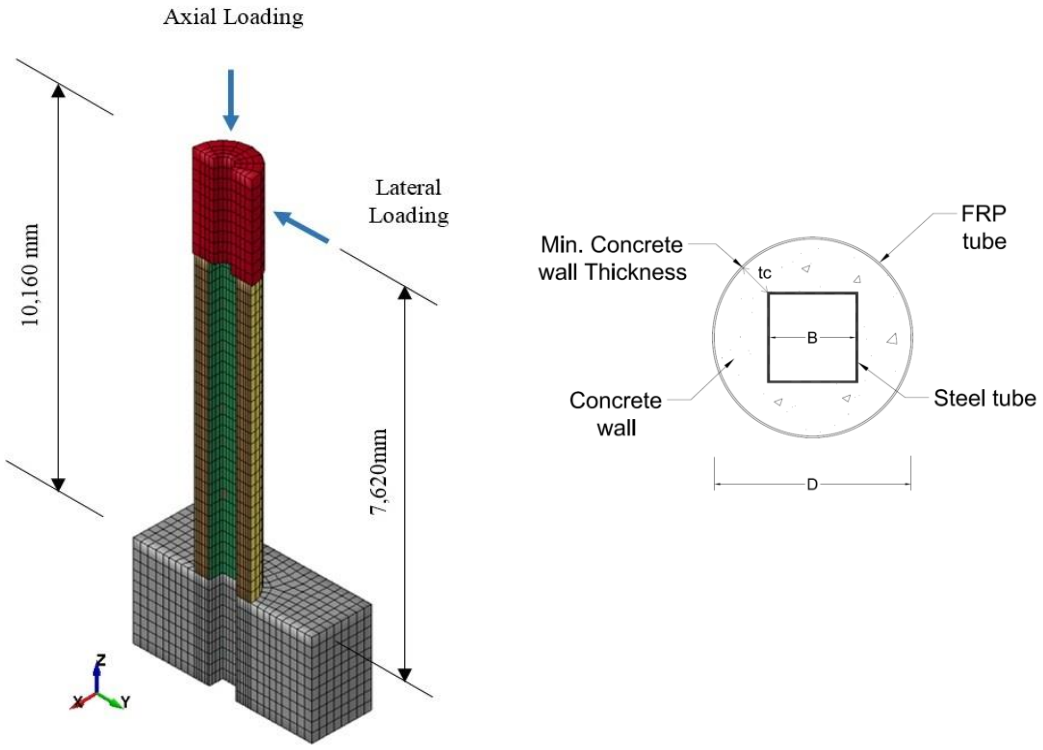

(a) (b)

Figure 3. FE model of the square HC-FCS columns (a) large scale model; (b) column's cross-section.

RESULTS AND DISCUSSION

This study found that the behavior of HC-FCS depends on the combination of stiffnesses of the three composite materials: FRP, steel, and concrete sandwiched between them. Strength and lateral displacement capacity of the investigated columns are illustrated in Figures 4, 5, and Table 2. These results revealed a conceptual base to understand the behavior of such columns.

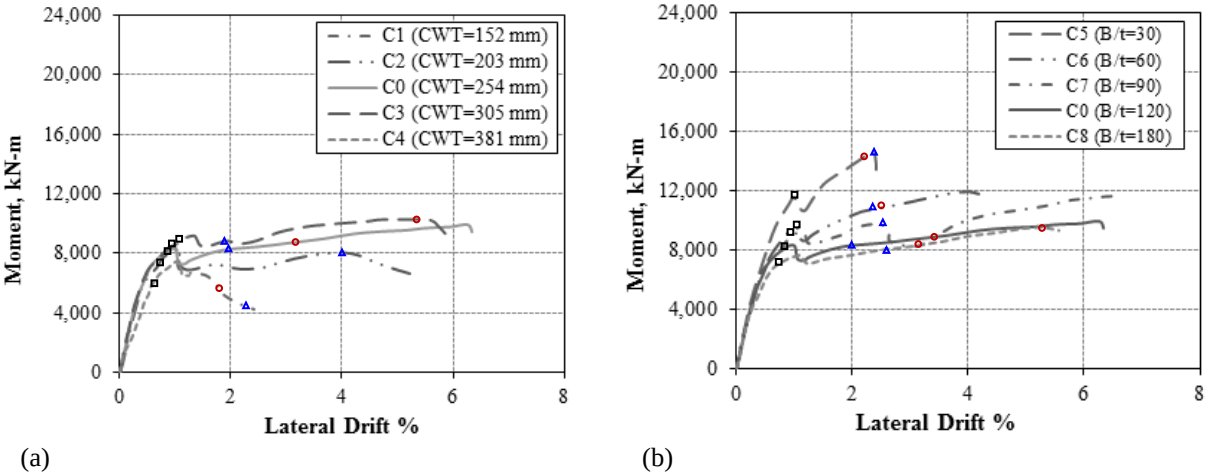

Figure 4. Moment versus lateral displacement capacity for HC-FCS columns (a) concrete wall thickness (CWT); (b) B/t ratio for the steel tubes.

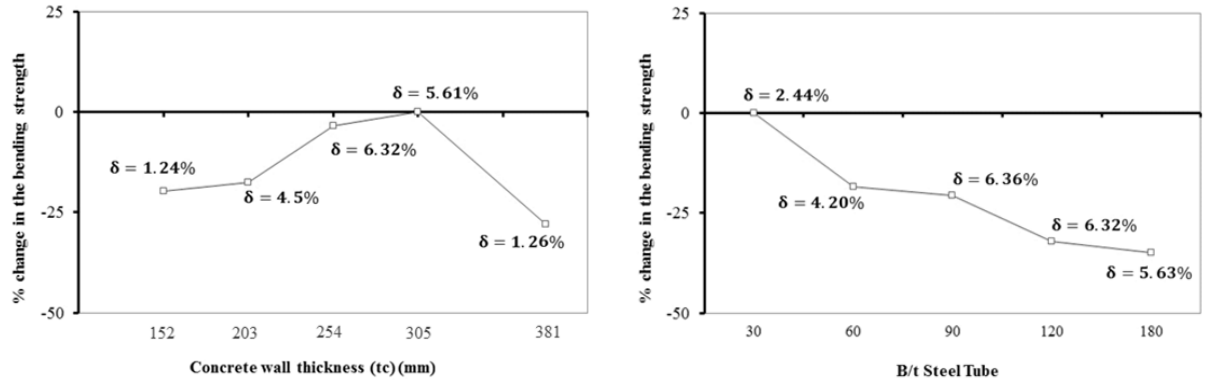

Figure 5. Percentage change in the bending strength and maximum lateral displacement capacity for (a) concrete wall thickness; (b) B/t for the steel tubes.

Table 2. Summary of the parametric study results

Group	Model Name	Details		FE results	
				Moment Capacity [kN-m]	Lateral Drift (%)
A	C1	Concrete Wall Thickness [mm], t_c	152	8,456	1.24
	C2		203	8,473	4.5
	C0		254	9,992	6.32
	C3		305	10,276	5.61
	C4		381	7,412	1.26
B	C5	B/t	30	14,700	2.44
	C6		60	11,991	4.2
	C7		90	11,669	6.36
	C0		120	9,992	6.32
	C8		180	9,556	5.63

EFFECT OF MIN. CONCRETE WALL THICKNESS

The effect of concrete wall thickness (CWT) [t_c in Table 1, 2 and Fig. 3 (b)] on HC-FCS columns was investigated by comparing the results of five columns with concrete wall thicknesses of 152.4 to 381 mm. Figure 4 (a), 5 (a), and Table 2 show that increasing the concrete wall thickness from 152.4 to 304.8 mm resulted in an increase in the bending strength capacity by 22%. The maximum lateral drift was 6.32%, achieved with a concrete wall thickness of 254 mm.

Changing the concrete wall thickness revealed complex nonlinear behavior for the columns. The square steel tubes reduced the concrete confinement due to the non-uniform distribution of the confining pressure that was highly concentrated at the corners [Fig.6 (a)]. The presence of concrete wall prevents the outward local buckling of the steel tube from happening, leading to only inward local buckling and thereby improving the flexural strength capacity of the investigated columns [Fig. 6 (b)].

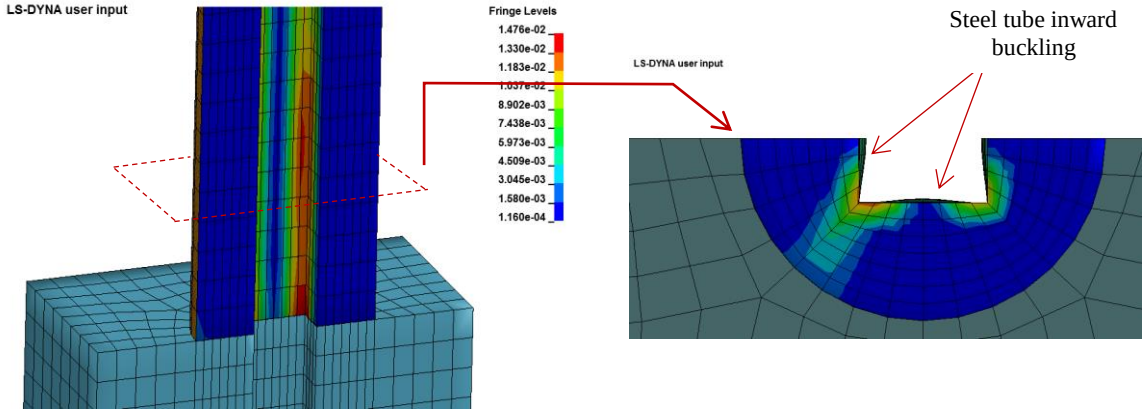

(a) (b)

Figure 6. Confining pressure distribution (a) concentrated at the corners, and (b) section view with the steel tube inward buckling.

EFFECT OF STEEL TUBE SLENDERNESS (B/T) RATIO

Five different square steel tubes with B value equal to 712 mm and B/t ratios of 30, 60, 90, 120, and 180 were used during this study to investigate the effects of the steel tubes slenderness ratios on both the lateral drift and strength capacity. Figure 4 (b), 5 (b), and Table 2 show an increase in the bending capacity by 154% (from 9,556 kN-m to 14,700 kN-m) as the B/t of the steel tube decreased by 83.3% (from 180 to 30). The lateral drift values were increased by 160% from 2.44% to 6.32% with the (B/t) ratio increased by 300% from 30 to 120 (Table 2). The maximum lateral drift was 6.36% obtained for column C7 (B/t=90) in group B. Generally, the buckling strength increased with increasing the steel tube thickness. The inward displacements of the square steel shell are due to the confined concrete wall lateral expansion (volume expansion) pressure on the steel tube face. In the case of column C5 with lowest B/t ratio of 30, the steel tube was able to reach the yield stress and then led to footing concrete crushing failure. This result of footing damage agreed with the experimental result presented by Abdelkarim et al. (2016) when they used steel tube with a diameter-to-thickness ratio of 32.

All the columns in Group B were susceptible to the local buckling effect in the inner steel tube when the B/t ratio increased. The localization of the buckling occurred at lateral drift 0.8%–1.5% within the bottom most 640 mm of the column.

LOCAL BUCKLING EVALUATION FOR HC-FCS

Local buckling developed in the steel tube as compressive stress-initiated complex phenomena cause a case of redistribution of the generated stresses. Thus, the large portion of these stresses due to the applied loads was carried near the junctions (corners) of the inner square steel tube.

Using the concept of the local buckling deformations of thin steel plate restrained by concrete (Uy and Bradford 1996; Uy 1998), two expressions (Table 3) were used to calculate the local buckling stresses for Group B of the HC-FCS columns (Table 1). The obtained results were then compared with those obtained from the FE, as shown in Table 4.

Table 3. Summary of the used expressions

Reference	Method	Expression
(Uy and Bradford 1996)	SAFSM	$F_{cr} = \frac{\pi^2 E_s}{12(1-v^2)} k\left({}^{t}/_{b}\right)^2$
(AISC 2010; Ziemian 2010)	Effective width (EWM)	$F_{cr} = \frac{9E_s}{\left({}^{b}/_{t}\right)^2}$

where F_{cr} is the buckling stress [MPa (ksi)], k is the buckling coefficient = 10.30 for sidewalls in concrete filled tubes, E_s is the elastic modulus [GPa], v is the Poisson's ratio, and ${}^{b}/_{t}$ is the steel slenderness ratio.

Table. 4 Summary of the calculated results

	F_{cr} [MPa]				
B/t ratio	FE	SAFSM	SAFSM/FE	EWM	EWM/FE
60	396	562.1	1.42	499.5	1.26
90	194	238.8	1.23	222	1.14
120	139	136.9	0.98	124.9	0.90
150	93.5	88.2	0.94	80	0.86
180	82.5	62.3	0.76	55.5	0.67

The FE model predicted the initial local buckling stress of the investigated columns at 635 mm bove the top footing level, which is consistent with the proposed expression by AISC (2010) and Uy and Bradford (1996) (Table 3).
A regression analysis was then performed on the calculated data, and the best fit was found to be given by the expression in Eq. (1) (Fig. 7):

$$F_{cr} = 1.82\, E_s \times \left({}^{b}/_{t}\right)^{-1.65} \quad (1)$$

where F_{cr} is the buckling stress [MPa (ksi)] of HC-FCS columns, E_s is the elastic modulus [GPa (10^3ksi)], and ${}^{b}/_{t}$ is the steel slenderness ratio.

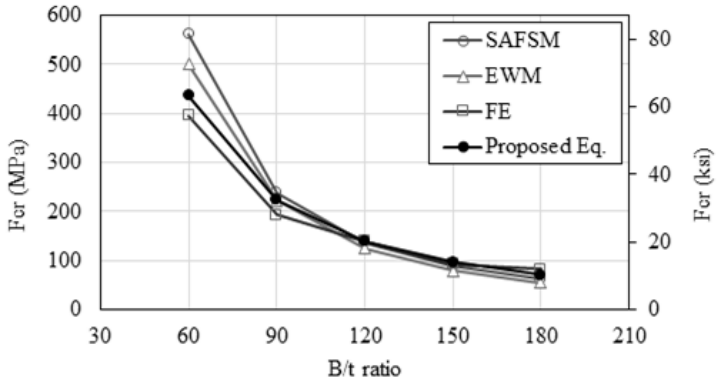

Figure 7. Buckling strength versus B/t ratios.

CONCLUSIONS

Based on the parametric study, observations, comparison, and the results demonstrated in this study, the following conclusions can be developed:

1. The presence of concrete wall prevents the outward local buckling of the steel tube from happening, leading to only inward local buckling, and thereby improving the flexural strength capacity of the investigated columns.
2. Increasing the steel tube thickness leads to an increase in the bending capacity for a specific inner diameter value. The HC-FCS columns were more susceptible to the local buckling effect in the inner steel tube when the B/t ratio increased.
3. The local buckling instability effect assessment is a crucial and complex phenomenon at the same time. The evaluation of the local buckling loads for HC-FCS columns was carried out by using the available empirical equation and then comparing with FE results.

REFERENCES

Abdelkarim, O. I., and ElGawady, M. A. (2014). "Analytical and Finite-Element Modeling of FRP-Concrete-Steel Double-Skin Tubular Columns." *Journal of Bridge Engineering*.

Abdelkarim, O. I., and ElGawady, M. A. (2016). "Behavior of hollow FRP–concrete–steel columns under static cyclic axial compressive loading." *Engineering Structures*, 123, 77-88.

Abdelkarim, O. I., ElGawady, M. A., Gheni, A., Anumolu, S., and Abdulazeez, M. (2016). "Seismic Performance of Innovative Hollow-Core FRP–Concrete–Steel Bridge Columns." *Journal of Bridge Engineering*, 04016120.

Abdelkarim, O. I., Gheni, A., Anumolu, S., Wang, S., and ElGawady, M. (2015). "Hollow-Core FRP-Concrete-Steel Bridge Columns Under Extreme Loading." *No. cmr 15-008*. 2015.

Abdulazeez, M. M., Abdelkarim, O. I., Gheni, A., ElGawady, M. A., and Sanders, G. (2017). "Effects of Footing Connections of Precast Hollow-Core Composite Columns." *Proc., Transportation Research Board (TRB) 96th Annual Meeting*, Transportation Research Board, Washington, DC.

AISC (2010). "Specification for structural steel buildings.", 360-10, Chicago.

Cheung, Y. (1976). "Finite strip method in structural mechanics." *Pergoman, New York, USA*.

Fam, A. Z., and Rizkalla, S. H. (2001). "Confinement model for axially loaded concrete confined by circular fiber-reinforced polymer tubes." *ACI Structural Journal*, 98(4).

Ozbakkaloglu, T., and Akin, E. (2011). "Behavior of FRP-confined normal-and high-strength concrete under cyclic axial compression." *Journal of Composites for Construction*, 16(4), 451-463.

Ozbakkaloglu, T., and Idris, Y. (2014). "Seismic behavior of FRP-high-strength concrete–steel double-skin tubular columns." *Journal of Structural Engineering*.

Shakir-Khalil, H., and Illouli, S. (1989). "Composite columns of concentric steel tubes."

Sheikh, S. A., and Yau, G. (2002). "Seismic behavior of concrete columns confined with steel and fiber-reinforced polymers." *ACI Structural Journal*, 99(1).

Teng, J., and Lam, L. (2004). "Behavior and modeling of fiber reinforced polymer-confined concrete." *Journal of structural engineering*, 130(11), 1713-1723.

Uy, B. (1998). "Local and post-local buckling of concrete filled steel welded box columns." *Journal of Constructional Steel Research*, 47(1), 47-72.

Uy, B., and Bradford, M. (1996). "Elastic local buckling of steel plates in composite steel-concrete members." *Engineering Structures*, 18(3), 193-200.

Von Karman, T., Sechler, E. E., and Donnell, L. (1932). "The strength of thin plates in compression." *Trans. ASME*, 54(2), 53-57.

Winter, G. (1970). "Commentary on the 1968 edition of the specification for the design of cold-formed steel structural members."

Wright, H. (1995). "Local stability of filled and encased steel sections." *Journal of structural engineering*, 121(10), 1382-1388.

Youssf, O., ElGawady, M. A., Mills, J. E., and Ma, X. (2014). "Finite element modelling and dilation of FRP-confined concrete columns." *Engineering Structures*, 79, 70-85.

Zhang, B., Teng, J., and Yu, T. (2012). "Behaviour of hybrid double-skin tubular columns subjected to combined axial compression and cyclic lateral loading."

Ziemian, R. D. (2010). *Guide to stability design criteria for metal structures*, John Wiley & Sons.